Bulk optical damage thresholds for doped and undoped, crystalline and ceramic yttrium aluminum garnet

Binh T. Do[1] and Arlee V. Smith[2,*]

[1]Ball Aerospace, Technologies Corporation, Albuquerque, New Mexico, USA 87106

[2]AS Photonics, Albuquerque, New Mexico, USA 87112

*Corresponding author: arlee.smith@as-photonics.com

Received 18 February 2009; revised 8 May 2009; accepted 29 May 2009;
posted 4 June 2009 (Doc. ID 107706); published 15 June 2009

We measured the bulk optical damage thresholds of pure and Nd-doped ceramic yttrium aluminum garnet (YAG), and of pure, Nd-doped, Cr-doped, and Yb-doped crystalline YAG. We used 9.9 ns, 1064 nm, single-longitudinal mode, TEM_{00} pulses, to determine that the breakdown thresholds are deterministic, with multiple-pulse thresholds ranging from 1.1 to 2.2 kJ/cm^2.

OCIS codes: 140.3330, 140.3530, 140.3615, 260.5950.

1. Introduction

Crystalline yttrium aluminum garnet (YAG) has long been an important laser host material because of its high thermal conductivity and high optical-damage threshold. Recently ceramic YAG has been developed to supplement crystalline YAG. It has advantages in fabrication of large amplifiers as well as in achieving high doping levels and variable doping profiles. There is little or no reduction in thermal conductivity or optical quality for the ceramic. It is of interest to compare its damage threshold with crystalline YAG. It also desirable to obtain reliable absolute values for the intrinsic damage thresholds of both materials.

Damage thresholds of undoped and 0.7% Nd-doped ceramic YAG have been reported by Bisson *et al.* [1]. They used 4 ns pulses of 1064 nm light to measure single-pulse damage and to find a statistical damage threshold at a fluence approximately 1/3 that of fused silica. However, their laser operated on multiple longitudinal modes, and this is known to produce a statistical variation of the apparent threshold [2]. In addition, the beam quality was relatively poor, with $M^2 \approx 2$. They report damage threshold fluences of $100 \pm 10\,J/cm^2$ for undoped ceramic and undoped crystalline YAG, and $110 \pm 10\,J/cm^2$ for Nd-doped ceramic and crystalline YAG. They attribute the observed statistical nature of breakdown to a statistical distribution of impurities in the samples, because the electron avalanche leading to optical breakdown was thought to start from seed electrons liberated from impurities.

Zelmon *et al.* [3] reported multiple-pulse damage thresholds for ceramic YAG by 8 ns pulses of multilongitudinal-mode, 1064 nm light. Their samples were doped 0–8% with Nd. They reported damage threshold irradiances of $50\,GW/cm^2$ ($400\,J/cm^2$) for doping levels 4% and less. At 8% doping, the crystal transparency was diminished, and the damage threshold was a factor of five lower.

Kamimura *et al.* [4] measured bulk damage thresholds for Nd-doped ceramic YAG using 8 ns, 1064 nm pulses. They claimed high-quality ceramic YAG has a damage threshold equal to crystalline YAG and approximately half that of silica. They did not report a dependence on doping level.

We have applied the techniques we developed for precise measurements of the damage threshold of silica [2] to measure damage thresholds of crystalline and ceramic YAG, and we find quite different behavior. We find that damage is deterministic rather than

0003-6935/09/183509-06$15.00/0

statistical for all of our YAG samples. Like silica, there is a well-defined single-pulse damage threshold. However, unlike silica, there is also a cumulative damage effect that leads to a reduced threshold for multiple pulses. Nevertheless, for any specific number of pulses there is a well-defined, deterministic damage limit. We find that undoped ceramic YAG has a higher threshold than undoped crystalline YAG. We also observe a substantial variation of thresholds for different dopants. We measure damage fluences substantially larger than those of Zelmon *et al.* [3] or Bisson *et al.* [1], with the lowest multiple-pulse limit being $1100\,\mathrm{J/cm^2}$ for Nd-doped ceramic YAG.

2. Experiment

Our measurement technique was described in detail in an earlier publication [2]. Briefly, we use single-longitudinal and transverse mode pulses focused to a small waist located well behind the front face of the sample. This prevents surface damage and also minimizes the influence of self focusing and stimulated Brillouin scattering (SBS), both of which depend on full beam power rather than the irradiance at the focus, and both of which can complicate the measurement of intrinsic damage thresholds. Damage is detected by a sudden, large loss in transmission of the 1064 nm beam, by a flash of white light emitted from the breakdown plasma, and by scattering of a He–Ne laser probe beam that overlaps the path of the 1064 nm beam. Fast vacuum phototubes record the incident and transmitted pump beams, a photomultiplier tube records the white light, and a white screen displays the transmitted He–Ne probe beam.

For the YAG measurements presented here, a fast shutter is used to pass a preselected number of pulses from the 10 pulses-per-second (pps) laser. We varied the pulse energy using a half-wave plate and a high-energy polarizer. The beam profile was nearly perfect $\mathrm{TEM_{00}}$, and the polarization was linear. The samples were mounted on a translation stage with $5\,\mu$m lateral resolution and 50 nm longitudinal resolution. The pulse duration was 9.9 ns FWHM. We focused the beam to an $8.1\,\mu$m waist (radius at $1/e^2$ irradiance) in the sample using a 25 mm focal length, best form lens, with antireflection coatings on both surfaces. Surface third harmonic was used to characterize the focus and also to position the sample input surface 3.7 mm in front of the beam waist. Damage locations were laterally separated by $600–800\,\mu$m.

We purchased our single-crystal YAG samples from United Crystals Co. They were cut for propagation of the light beam along the ⟨111⟩ crystallographic direction. This is a commonly used cut for YAG lasers. The ceramic YAG was purchased from Baikowski USA. Its micro crystalline grains are randomly oriented, with a mean size of $10–20\,\mu$m. The Rayleigh range of the focus was $350\,\mu$m so the focus spanned many such grains. The doping levels are 0.7% for Nd (ceramic and crystalline) and 8% for Yb, while the Cr-doped sample is sold as a passive Q switch with a 0.2% (atomic) doping.

3. Results

All of the tested samples exhibited distinctly different single-pulse and multiple-pulse damage thresholds, as shown in Fig. 1. For example, in undoped crystalline YAG the single-pulse damage threshold fluence was approximately $1400\,\mathrm{J/cm^2}$. At fluences of $1360–1400\,\mathrm{J/cm^2}$, the sample always damaged on the second pulse, while at $1316\,\mathrm{J/cm^2}$ the crystal damaged on either the third or fourth pulse, and at $1184\,\mathrm{J/cm^2}$ an unlimited number of pulses failed to cause damage. Figure 2 shows the time of breakdown versus fluence as the fluence is increased from the single-pulse threshold of $1400\,\mathrm{J/cm^2}$ up to $2200\,\mathrm{J/cm^2}$. As the fluence increases, the onset of damage occurs progressively earlier in the pulse. In contrast, breakdown in the multiple-pulse range always occurs near the peak of a pulse, never on the trailing edge. Qualitatively similar behavior was observed for all samples but at differing fluence levels. We found no variation of the damage properties in the crystalline samples when the polarization direction of the linearly polarized light was varied relative to the crystallographic axes. All of the fluences shown in Figs. 1 and 2 are uncorrected for self focusing. We discuss this correction below.

Clearly, the samples accumulate some sort of material modification before actual breakdown for fluences lying in the multipulse threshold zone. This modification appears to be permanent because the multiple-pulse thresholds do not depend on the pulse repetition rate over the range 10 to 0.01 pps. We notice a slight, progressive reduction in transmission of the 1064 nm light associated with this accumulation. However, we can find no indication of it by examination with a phase contrast microscope, nor is there noticeable change in the mode profile of the transmitted He–Ne probe beam.

Damage morphology is similar to that in silica. For a pulse energy slightly above the single-pulse threshold, damage occurs along a thin line centered on the focal waist and has a length of approximately 1/3 the Rayleigh range. When the pulse energy is increased by 30%, the damage is further extended by approximately another 1/3 of the Rayleigh range, but only in the upstream direction.

The white light emission from the breakdown plasma is also similar to that in silica, with a prompt 20–30 ns pulse and a much longer and weaker tail. The white light time profiles are reproducible, and are slightly different for crystalline and ceramic samples.

Such deterministic damage with different fluence thresholds for different numbers of pulses is similar to that reported by Maldutis [5] for K8 crown glass damaged by nanosecond pulses at 1064 nm, and by Mero *et al.* [6] for $\mathrm{Ta_2O_5}$ films damaged by femtosecond pulses at 800 nm.

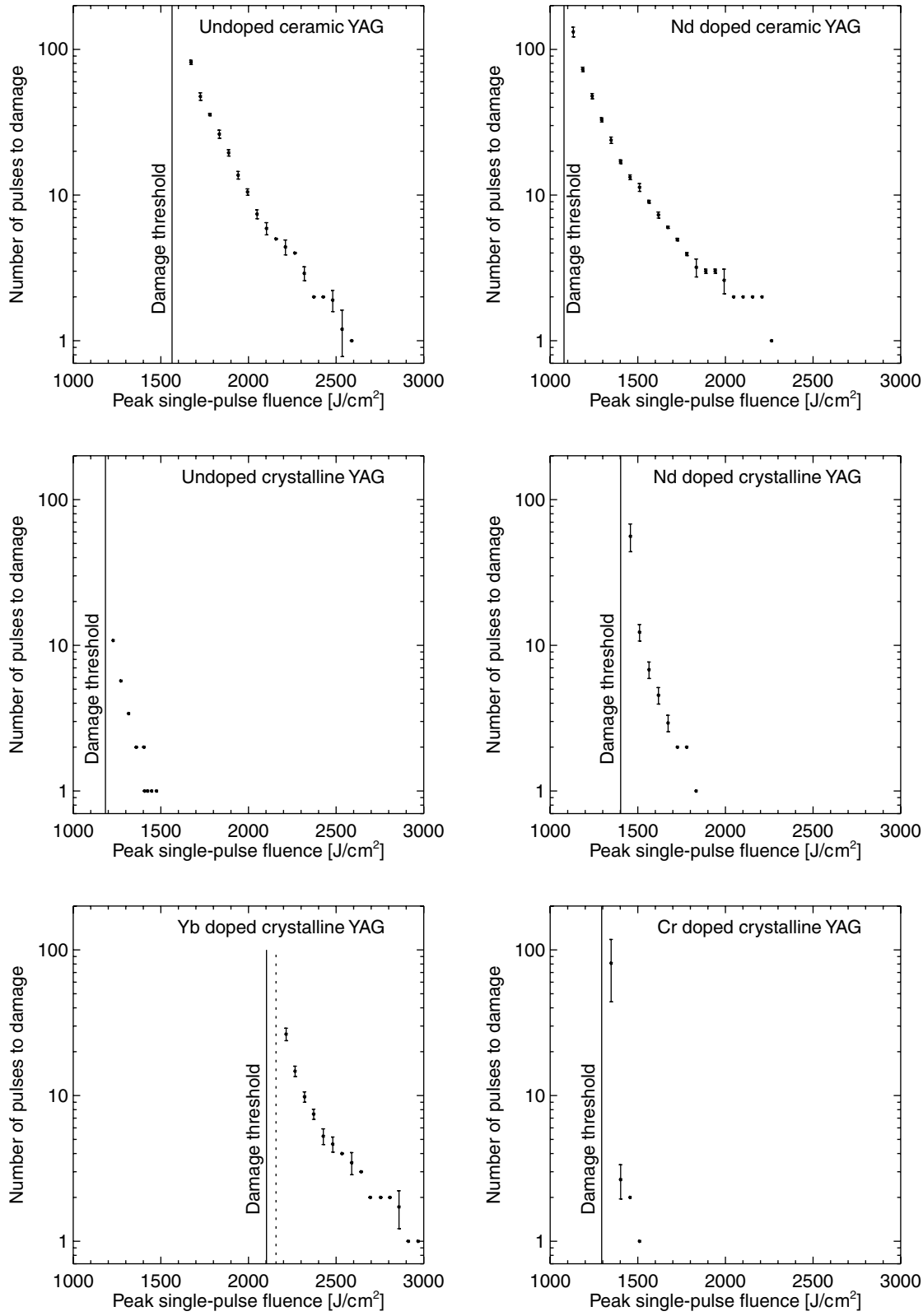

Fig. 1. Number of pulses required to damage various YAG samples versus the single-pulse fluence for 9.9 ns, 1064 nm pulses. These fluences are not corrected for self focusing.

The high Yb doping concentration (8%) in our Yb-doped crystals evidently creates substantial internal stress because the small fractures produced by optical damage grow within a few hours to extend throughout the crystal. Our measurements were made quickly, before the fractures grew significantly.

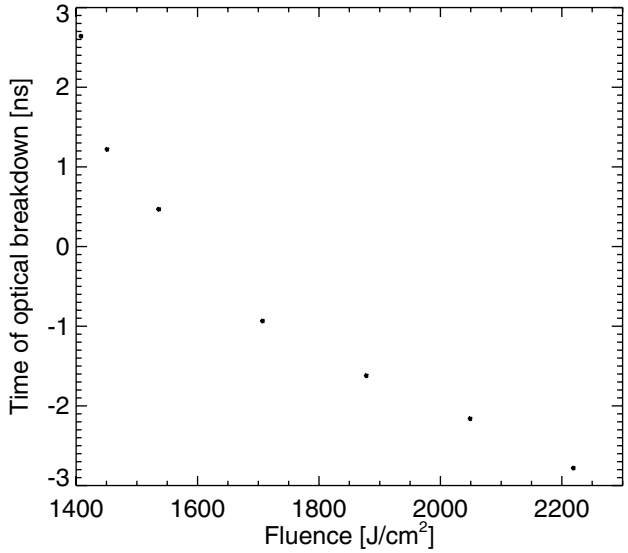

Fig. 2. Time of single-pulse breakdown in crystalline, undoped YAG relative to the center of the pulse (time = 0) as a function of peak onaxis fluence. These fluences are not corrected for self focusing.

There is some spread in the lowest damage threshold for these crystals. Crack growth does not occur in the other samples.

The Cr-doped samples absorb 1064 nm light due to a Cr^{+4} absorption cross section of $5 \times 10^{-18}\,cm^2$ and a doping density of approximately $3 \times 10^{17}\,cm^{-3}$. However, this absorption is strongly bleached even by the minimum damage threshold photon fluence of $8 \times 10^{21}\,cm^{-2}$. Bleaching is known to be polarization dependent [7], but this effect is minimized by orienting the crystal for propagation along the ⟨111⟩ crystallographic direction.

4. Analysis

Two effects that must be accounted for when analyzing bulk damage threshold measurements are self-focusing and SBS.

A. Self-Focusing Correction

As is well known, there is a critical self-focusing power for a Gaussian beam, defined by

$$\mathcal{P}_{SF} = \frac{0.148\lambda^2}{nn_2}, \tag{1}$$

where n_2 is in units of m^2/W. Adair *et al.* [8] reported that n_2 of fused silica is 3.18 ± 0.15 times smaller than that of crystalline YAG for linearly polarized, 1064 nm light. Their method excluded electrostrictive contributions to n_2. Based on the accepted value of the Kerr contribution to n_2 for silica of $2.23 \times 10^{-20}\,m^2/W$, this implies a Kerr contribution to the nonlinear index of YAG equal to $6.7 \pm 0.6 \times 10^{-20}\,m^2/W$. This corresponds to a critical self-focusing power of 1.4 MW for linearly polarized, 1064 nm light.

However, our relatively long 9.9 ns pulses and small focal waist do allow electrostrictive contributions to n_2, so we will estimate this contribution. The electrostrictive portion of n_2 satisfies [9]

$$n_2 \propto \beta\left(\rho\frac{dn}{d\rho}\right)^2, \tag{2}$$

where β is the compressibility of YAG. The compressibility ratio of silica to YAG is of order unity, and, according to Wexler [9], the value of the quantity in parentheses is –0.01 for YAG, compared to 0.32 for fused silica, so the electrostrictive n_2 is roughly a factor of 1000 smaller for YAG than silica. Considering that electrostriction accounts for only 20% of n_2 in silica, we can safely ignore its contribution for YAG.

We must also take into account the anisotropy of n_2. The crystal structure of YAG is cubic with point group $m3m$. In crystals of this symmetry, the Kerr contribution to n_2 for linearly polarized light is independent of polarization direction for light propagating along the ⟨111⟩ direction [10], if we assume Kleinman symmetry, which asserts $\chi^{(3)}_{ijji} = \chi^{(3)}_{iijj}$. Further, under Kleinman symmetry the relative contributions to n_2 from $\chi^{(3)}_{xxyy}$ and $\chi^{(3)}_{xxxx}$ are 3 to 1. These two contributions are individually independent of the polarization direction. If $\chi^{(3)}_{xxxx}/\chi^{(3)}_{xxyy} = 3$, the contributions are equal and the Kerr response is identical for all propagation angles, making self focusing identical in all directions for all polarization directions, just as in an isotropic medium such as fused silica. Evidently this 3∶1 ratio is nearly correct. According to Owyoung [11] the self-focusing critical power for light polarized along the [100] direction is 96% of that for light polarized along [110]. Assuming Kleinman symmetry, this ratio implies $\chi^{(3)}_{xxxx}/\chi^{(3)}_{xxyy} = 3.26 \pm 0.10$. We conclude that the critical self-focusing power should depend only weakly on the propagation and polarization directions, and $n_2 = 6.7 \times 10^{-20}\,m^2/W$ should apply to randomly-oriented crystals as well as crystals oriented for ⟨111⟩ propagation.

For a deep focus the irradiance at the highest irradiance point is increased by self focusing according to

$$I = \frac{I_o}{1 - \mathcal{P}/\mathcal{P}_{SF}}. \tag{3}$$

With this self-focusing correction integrated over the Gaussian temporal profile, the ceramic single- and unlimited multiple-pulse YAG threshold fluences of 2500 and $1550\,J/cm^2$ increase to 2860 and $1690\,J/cm^2$. Similarly, the two fluences for crystalline YAG increase from 1400 and $1180\,J/cm^2$ to 1505 and $1250\,J/cm^2$.

The small absorption mentioned above in connection with multiple-pulse damage could also cause self focusing. If it were due to linear absorption over the full length of the beam, this thermal self focusing would affect the focus if the absorption coefficient

were greater than $1\,\mathrm{cm}^{-1}$. In fact, the absorption is probably confined to a region within one Rayleigh range of the focus, in which case the self-focusing effect is minimized. Our analysis of thermal lensing indicates that it should not significantly affect the damage thresholds we are reporting.

B. SBS Threshold

For a Gaussian profile beam focused deep in the sample, there is a well-defined SBS threshold power, $\mathcal{P}_{\mathrm{SBS}}$. In silica we measured $\mathcal{P}_{\mathrm{SBS}} = 0.85\,\mathrm{MW}$ for an 8 ns pulse of 1064 nm light. The threshold power should scale as $1/g_B$, where g_B is the Brillouin gain coefficient that accounts for the pulse duration and acoustic lifetime. The physical mechanism responsible for SBS is the same one responsible for the electrostrictive contribution to n_2, so we anticipate a much higher SBS threshold for YAG than silica. The SBS gain coefficient satisfies [12]

$$g_B = \frac{k_s k_a n_s n_p p'^2}{2c\rho v_a \Gamma_B}, \tag{4}$$

where subscripts a, s, and p refer to acoustic, Stokes, and pump waves, respectively, v_a is the acoustic velocity, and Γ_B is the acoustic decay rate. The p' is the longitudinal elasto-optic coefficient, which is 0.01 for YAG and 0.27 for silica [13]. Similar values for these coefficients were used by Wexler [9] to compute the electrostrictive contribution to n_2 presented above. We conclude that $\mathcal{P}_{\mathrm{SBS}}$ is approximately 1000 times larger in YAG than in silica, assuming the net contribution from the other factors in g_B is of order unity. We conclude that the SBS threshold for YAG should be far higher than its damage threshold powers. In fact, we monitored the beam reflected from our samples, looking for evidence of SBS, but observed none throughout our YAG damage studies. This method gave a clear SBS signal for silica.

5. Damage Mechanism

Damage by nanosecond light pulses is usually attributed to a combination of multiphoton ionization and avalanche ionization caused by heating of conduction band electrons by the optical electric field. If the free electron density reaches approximately $2 \times 10^8\,\mu\mathrm{m}^{-3}$, the plasma frequency equals the optical frequency and the sample becomes highly absorbing. The deposited energy melts and fractures the material. The growth of conduction band electrons is often be modeled by a rate equation of the form

$$\frac{dn}{dt} = \beta I^k + \alpha n I - \frac{n}{\tau_r}, \tag{5}$$

where β is a multiphoton ionization coefficient for six photon ionization (the band gap of YAG is approximately 6.5 eV), α is an electron avalanche coefficient, and τ_r is an electron recombination lifetime.

Such a model can successfully account for the data of Fig. 2 by using a recombination time of approximately 3 ns and nearly equal contributions from multiphoton and avalanche ionization. However, this model does not account for the long-lived damage that accumulates over multiple pulses in multiple-pulse breakdown, so additional physical processes must be involved. Mero *et al.* [6] found similar multiple-pulse behavior for femtosecond damage of dielectric thin films. They ascribed the cumulative damage to populating a limited number low-lying, long-lived, self-trapped exciton states that ionize more readily than the valence electrons. They successfully modeled measured damage behavior using picosecond decay rates for conduction band electrons into these levels. This rate was comparable to that for decay into the valence band, so a substantial fraction of the electrons were liberated by photoionization/avalanche decay into these states. The trapped-state population builds up over many pulses until it fills nearly all the available traps. This saturation of the trap population is associated with the limited threshold reduction for multiple-pulse damage, compared with single-pulse damage. Clearly, in YAG there must also be some sort of long-lived states that are populated by the sub single-pulse threshold pulses. However, lacking independent evidence for the existence and nature of these states, we have not attempted to construct such a rate equation model.

Another striking feature of our results is that undoped ceramic YAG has a substantially higher damage limit than undoped crystalline YAG. As we discussed above, this cannot be accounted for by different self focusing or SBS properties. It could be due to higher breakdown thresholds for crystallite orientations different from the ⟨111⟩ direction of our crystalline samples. However, such variations should lead to considerable scatter in the damage limits for ceramic samples due to the limited number of crystallites in the focal volume. We do not see such variations from one location to another. The only reasonable explanation seems to be that the nature of the long-lived states or the rates for ionization and recombination are markedly different in the two materials, but that they are quite homogeneous across the crystallites in ceramic YAG.

In conclusion, the damage threshold of YAG is nearly five times lower than the threshold for silica, a larger difference than the factor of two found by Zelmon *et al.* [3] and Kamimura *et al.* [4]. Further, the considerable variation in YAG damage threshold with doping is a new observation.

This work was supported by the United States Department of Energy (DOE) under contract DE-AC04-94AL85000. Sandia is a multiprogram laboratory operated by Sandia Corporation, a Lockheed Martin Company, for the United States Department of Energy.

References

1. J. Bisson, Y. Feng, A. Shirakawa, H. Yoneda, J. Lu, H. Yagi, T. Yanagitani, and K. Ueda, "Laser damage threshold of ceramic YAG," Jpn. J. Appl. Phys. **42**, L1025–L1027 (2003).

2. A. Smith and B. Do, "Bulk and surface laser damage of silica by picosecond and nanosecond pulses at 1064 nm," Appl. Opt. **47**, 4812–4832 (2008).
3. D. E. Zelmon, K. L. Schepler, S. Guha, D. Rush, S. M. Hegde, L. P. Gonzales, and J. Lee, "Optical properties of Nd-doped ceramic yttrium aluminum garnet," Proc. SPIE **5647**, 255–264 (2005).
4. T. Kamimura, Y. Kawaguchi, T. Arii, W. Shirai, T. Mikami, T. Okamoto, Y. L. Aung, and A. Ikesue, "Investigation of bulk laser damage in transparent YAG ceramics controlled with micro-structural refinement," Proc. SPIE **7132**, 713215 (2008).
5. E. K. Maldutis, "Scaling in damage of optical materials by intensive laser radiation," Proc. SPIE **6720**, 672018 (2007).
6. M. Mero, B. Clapp, J. C. Jasapara, W. Rudolph, D. Ristau, K. Starke, J. Kruger, S. Martin, and W. Kautek, "On the damage behavior of dielectric films when illuminated with multiple femtosecond laser pulses," Opt. Eng. **44**, 051107 (2005).
7. H. Eilers, K. R. Hoffman, W. M. Dennis, S. M. Jacobsen, and W. M. Yen, "Saturation of 1.064 μm absorption in Cr, Ca: $Y_3Al_5O_{12}$ crystals," Appl. Phys. Lett. **61**, 2958–2960 (1992).
8. R. Adair, L. L. Chase, and S. A. Payne, "Nonlinear refractive index of optical crystals," Phys. Rev. B **39**, 3337–3350 (1989).
9. R. M. Wexler, "Laser glass composition and the possibility of eliminating electrostrictive effects," IEEE J. Quantum Electron. **7**, 166–167 (1971).
10. R. W. Boyd, *Nonlinear Optics*, 2nd ed. (Academic, 2003).
11. A. Owyoung, "Ellipse rotation studies in laser host materials," IEEE J. Quantum Electron. **9**, 1064–1096 (1973).
12. G. W. Faris, L. E. Jusinski, and A. P. Hickman, "High-resolution stimulated Brillouin gain spectroscopy in glasses and crystals," J. Opt. Soc. Am. B **10**, 587–599 (1993).
13. R. W. Dixon, "Photoelastic properties of selected materials and their relevance for applications to acoustic light modulators and scanners," J. Appl. Phys. **38**, 5149–5153 (1967).